Supplement of Atmos. Chem. Phys., 25, 16511–16532, 2025 https://doi.org/10.5194/acp-25-16511-2025-supplement © Author(s) 2025. CC BY 4.0 License.





Supplement of

Mount Pinatubo's effect on the moisture-based drivers of plant productivity

Ram Singh et al.

Correspondence to: Ram Singh (ram.bhari85@gmail.com)

The copyright of individual parts of the supplement might differ from the article licence.

S1. Baseline period selection

The requirement of a baseline time selection points towards a precise representation of climate conditions over a historical period, especially towards the later part of the 20th century, and sufficiently long enough for the calibration of drought indices. Figure S1 compares seasonal surface temperature responses in 1992 with respect to three selected base climate periods. It clearly shows that seasonal surface temperature is considerably influenced by the dominance of no anthropogenic forcing period (1850-2014 and 1920-1960). Consideration of the entire historical (1850-2014) and volcanically quiescent time-slice (1920-1960) as a base period result in the biasing of the reference climate towards the non-anthropogenic emission era.

Consequently, the volcano-induced signal due to the Mt. Pinatubo eruption gets muted by the response due to anthropogenic forcings. This influence is minimal with respect to the base period of 1950-2014, as this period mostly covers the period of anthropogenic signal emergence, and its length is sufficient for calibration statistics for SMDI and ETDI (As shown in Figure S1).

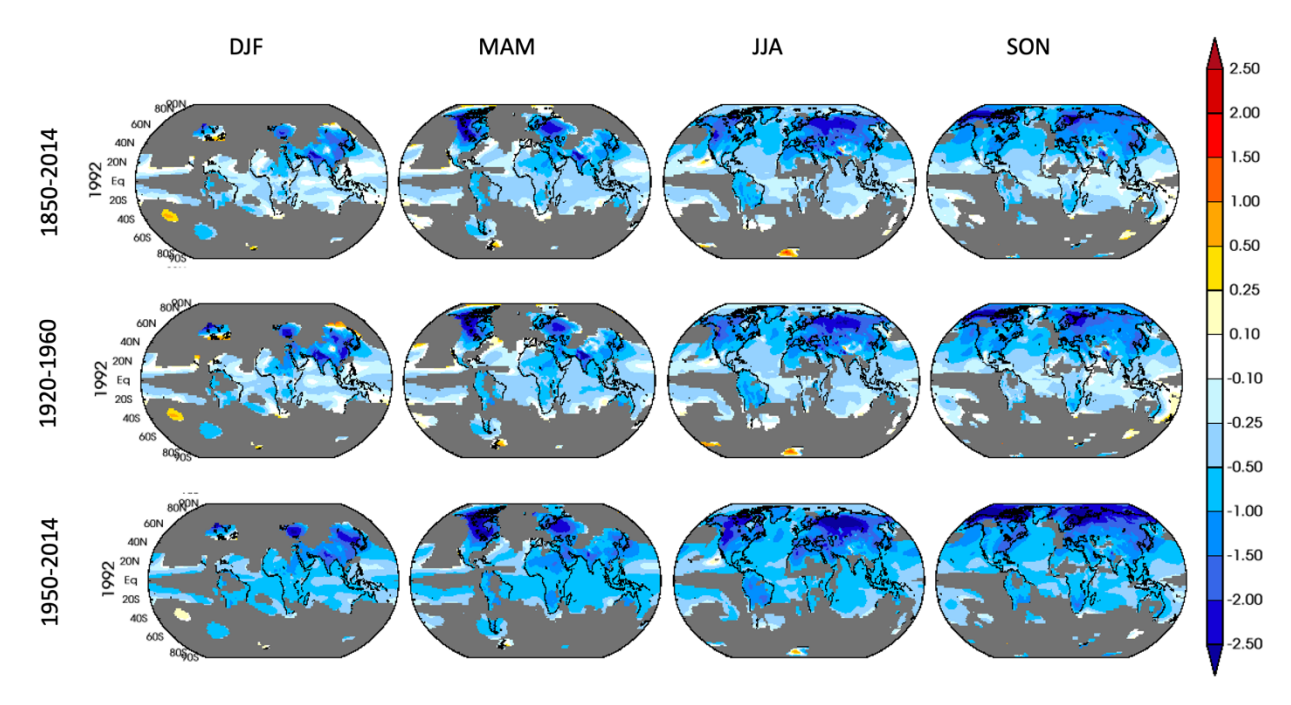


Figure S1. Seasonal surface temperature anomaly (multi-ensemble mean) for the year 1992 with respect to three different reference (base) time periods (row-wise).

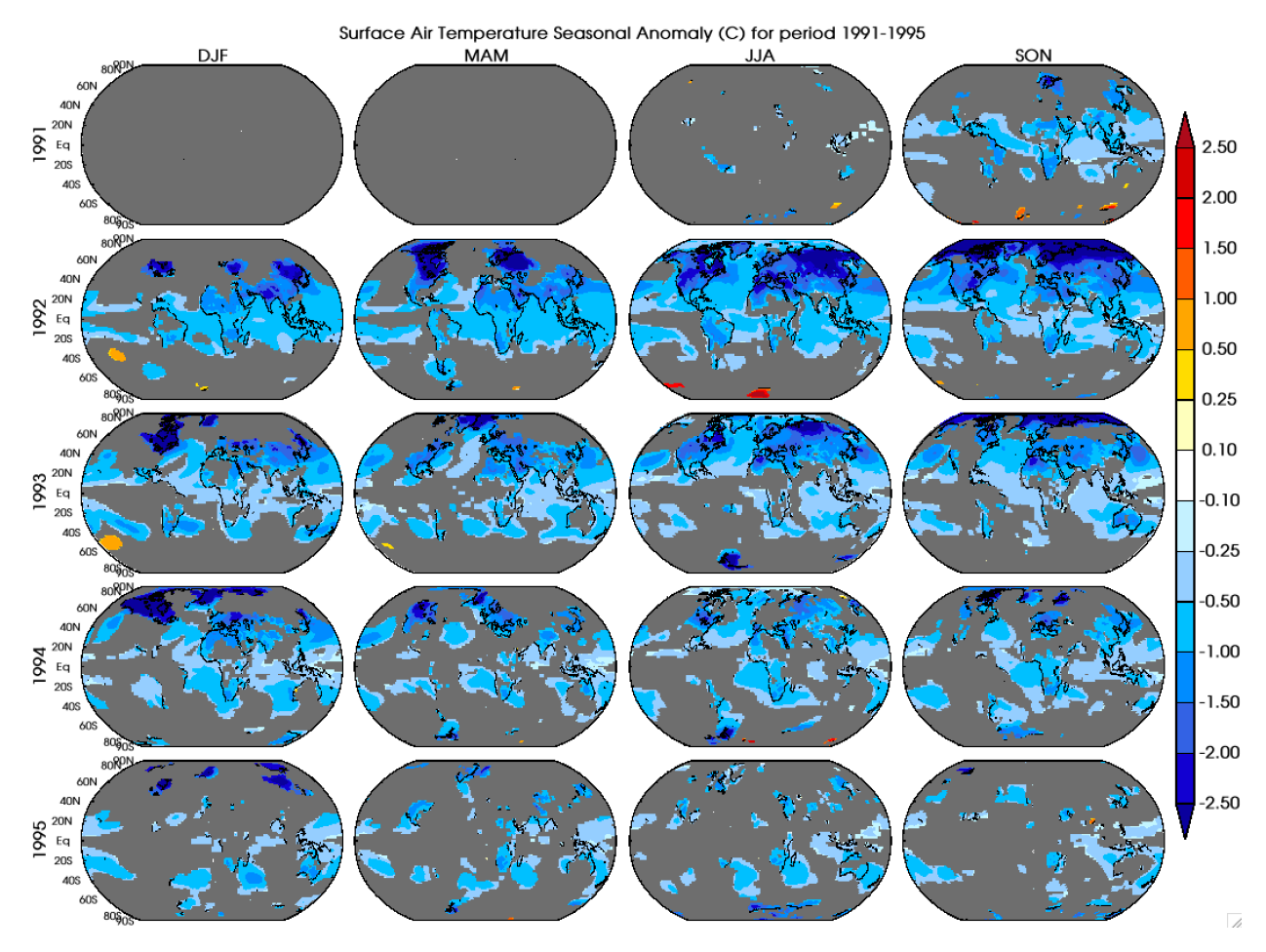


Figure S2. Surface temperature difference (°C) between the Pinatubo and No-Pinatubo (NP) ensemble from the year 1991 to 1995 for each season.

S2. Microphysical properties and radiative response

We analyze the microphysical properties of volcanic aerosol simulated by the NASA GISS ModelE (MATRIX) in the PCH ensemble set. The current setup of GISS ModelE uses the aerosol microphysical module MATRIX to represent the various states and provide particle number, mass, and size information for different mixed modes of the aerosol population. Sulfate aerosols grow by condensation of gas (nucleation and self-coagulation (preexisting)) to the Aitken (AKK) mode (mean mass diameter $<0.1~\mu m$), and further growth in size leads to the transfer to Accumulation (ACC) mode (Bauer et al., 2008; Bekki, 1995). The transfer between the two particle modes is controlled through the transfer function based on particle mean mass diameter (Bauer et al., 2008).

GISS ModelE (MATRIX) PCH simulated a sulfate aerosol size with an effective radius ($R_{\rm eff}$) of the order of 0.3-0.6 µm after the Mt. Pinatubo eruption (not shown), consistent with several observation and modeling estimates (Bauman et al., 2003; Bingen et al., 2004; Russell et al., 1996; Stenchikov et al., 1998). Quaglia et al. (2023) have presented a detailed evaluation of the control of aerosol injection strength and altitude on microphysical properties of volcanic aerosols using models with interactive chemistry and microphysics under the Interactive Stratospheric Aerosol Model Intercomparison Project (ISA-MIP). Broadly, ModelE (with the MATRIX aerosol microphysics code) simulated well the evolution of the volcanic plume (AOD, effective radius, and aerosol dispersion) compared to the closest match to our configuration of a sulfur injection strength ($\sim 7~TgS = 14~Tg$ of SO2) at injection heights both at 22km and the range 22-25 km presented by (Quaglia et al., 2023).

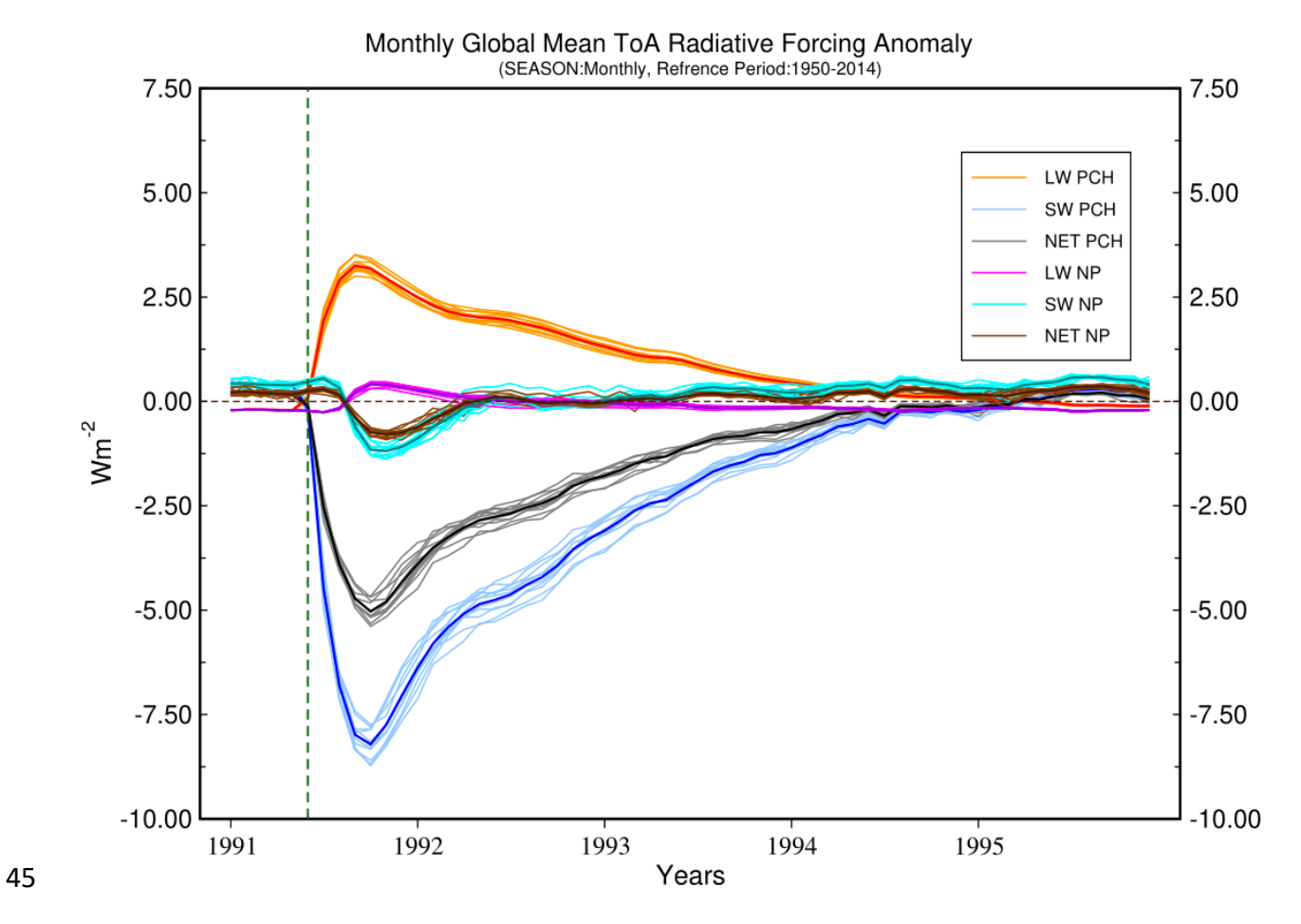


Figure S3. Monthly anomaly of longwave (LW), shortwave (SW), and net (NET) radiative forcing simulated by the GISS ModelE for Mt. Pinatubo (PCH) and without Pinatubo (NP) ensembles. The response anomalies are calculated with respect to the climatology for the period 1950-2014, taken from the GISS historical runs (GISS-HIST-SO2). The light-colored thin lines represent the individual ensemble member, and the dark broad line is the multi-ensemble mean for each variable (longwave, shortwave and net radiative response).



46

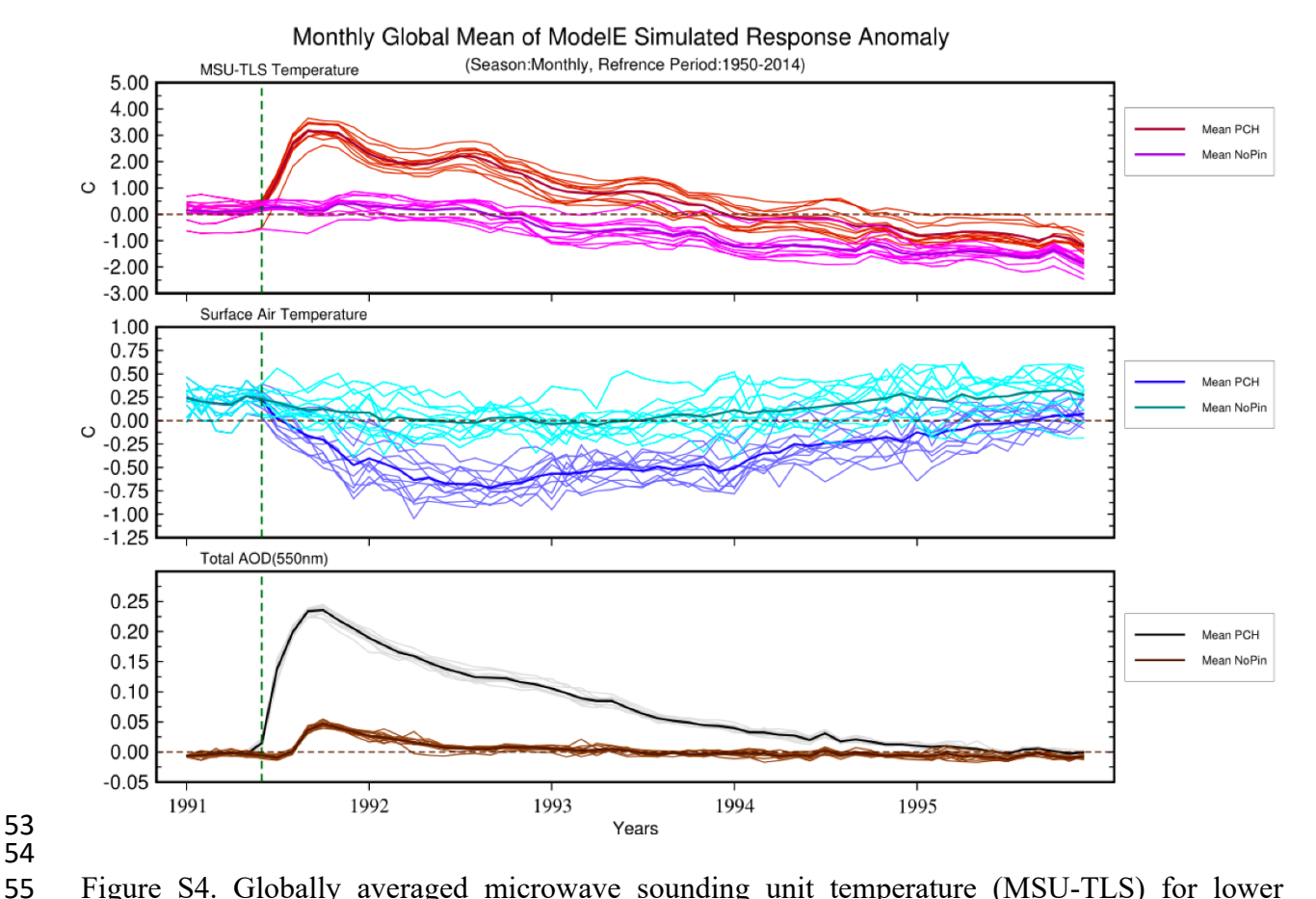
47

48

49

50

51



53 54

56

57 58 59

60

61

62

Figure S4. Globally averaged microwave sounding unit temperature (MSU-TLS) for lower stratosphere, surface temperature and total aerosol optical depth (AOD) at 550 nm wavelength response with respect to 1950-2014 as the reference period.

S3. Lower stratosphere response

The model simulates a peak warming of over 4 °C in the tropical lower stratosphere (MSU-TLS: microwave sounding unit temperature of lower stratosphere) shortly after the eruption, which lasts for a few months when the concentration of sulfate aerosols is highest (not shown here).

Significant warming in the range of 2-3 °C lasted until the end of 1992, and overall simulated stratospheric warming is consistent with previous studies. Figure S4 (top panel) shows a steplike transition with time with a global mean increase of 3.0 °C in the lower stratosphere temperature after the Mt. Pinatubo eruption, followed by a trend consistent with (Ramaswamy et al., 2006). The zonal structure of surface temperature shows that the surface cooling follows the aerosol optical depth pattern, and the most significant cooling is simulated in high latitudes. The temporal patterns of lower stratosphere warming and surface cooling reflect seasonal variations in incoming solar radiation over the northern polar latitudes.

S4. Rainfall response

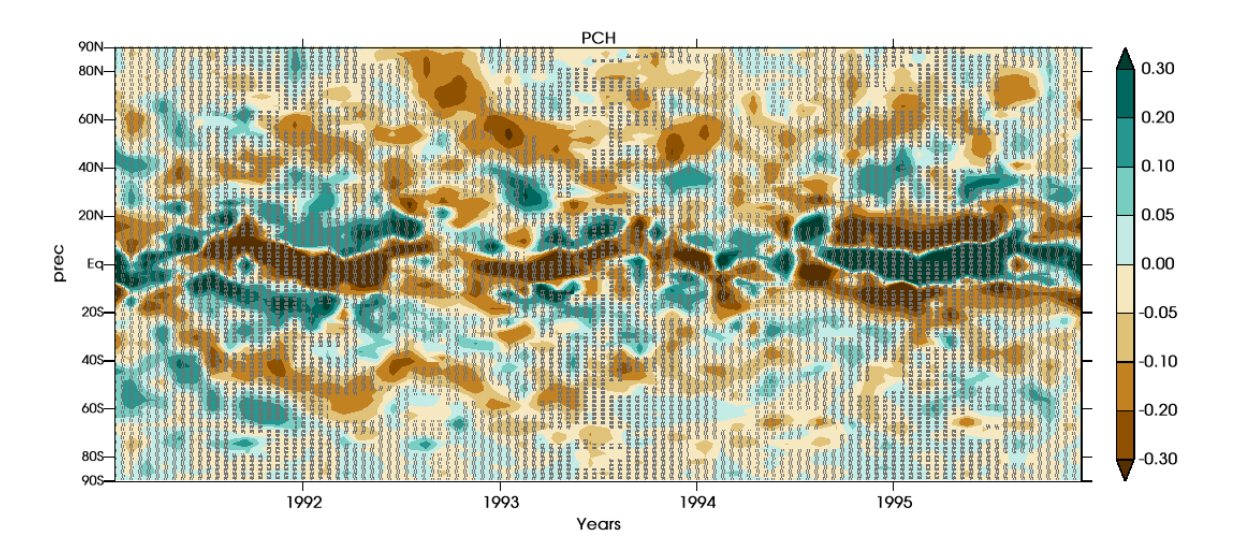


Figure S5. Zonal mean anomaly of rainfall response (mm/day) after the 1991's Mt. Pinatubo eruption. Grey colored stippling marks the statistically non-significant rainfall signal in comparison to the No Pinatubo (NP) ensemble.

(Colose et al., 2016) have postulated that the asymmetrical surface cooling and radiative balance perturbation create an energetical deficit in the hemisphere of eruption and consequently, it constrains the poleward propagation of tropical rainfall belt (ITCZ) in that hemisphere. The

zonal mean of the rainfall response (Figure S5) shows a clear decreasing trend in the northern hemisphere tropical and higher latitudes with a positive rainfall response band around $20^{\circ}~N$.

S5. SMDI (4-6 feet) and transpiration change

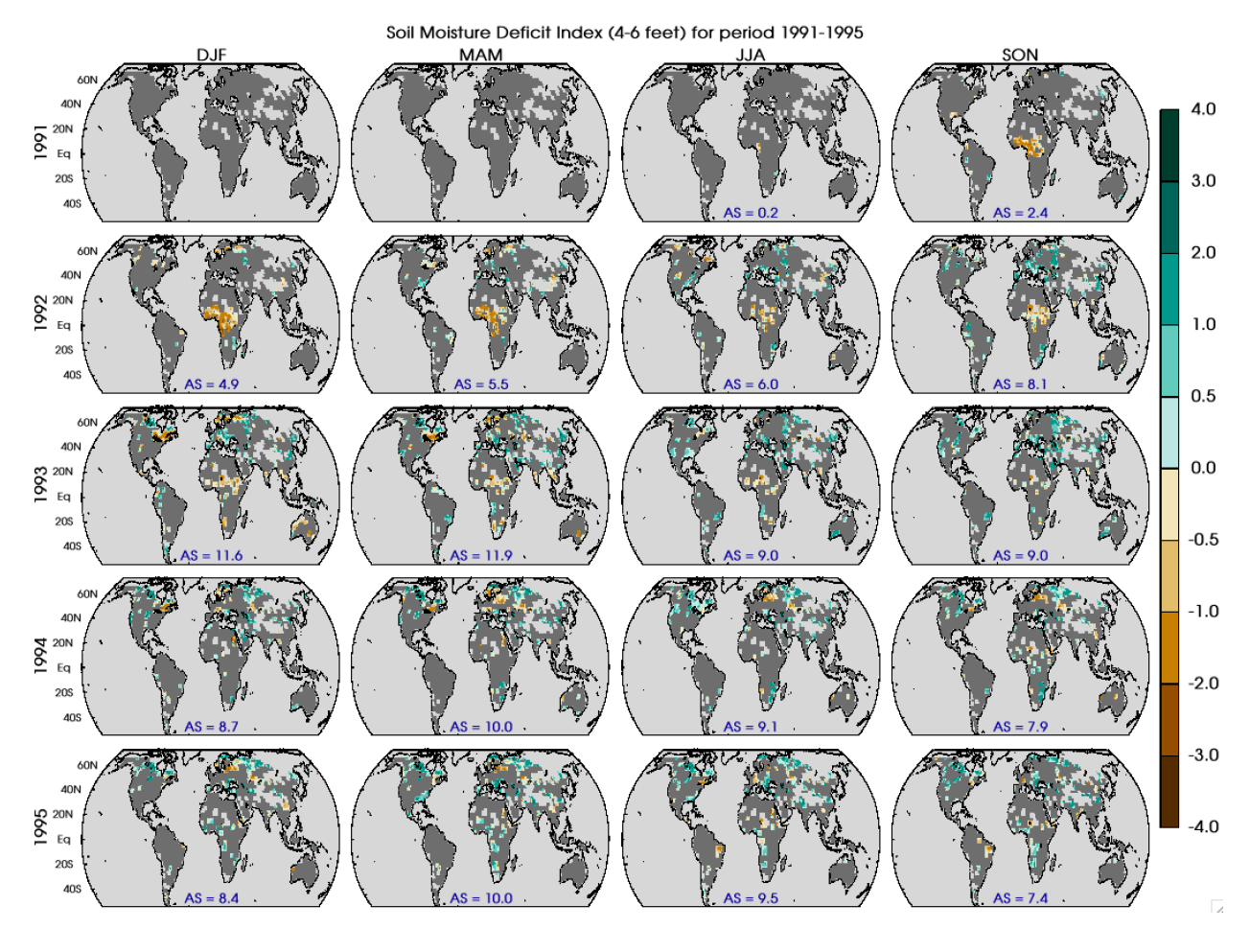


Figure S6. Soil moisture deficit index (SMDI_6) for the 4-6 feet depth of soil at seasonal scale from the year 1991 to 1995. Grey color is painted over the grid cells where the SMDI_6 is not statistically significant in contrast to No Pinatubo (NP) ensemble. The parameter AS on each panel marks the percentage of land area which shows a statistically significant dry or wet response after the Mt. Pinatubo eruption.

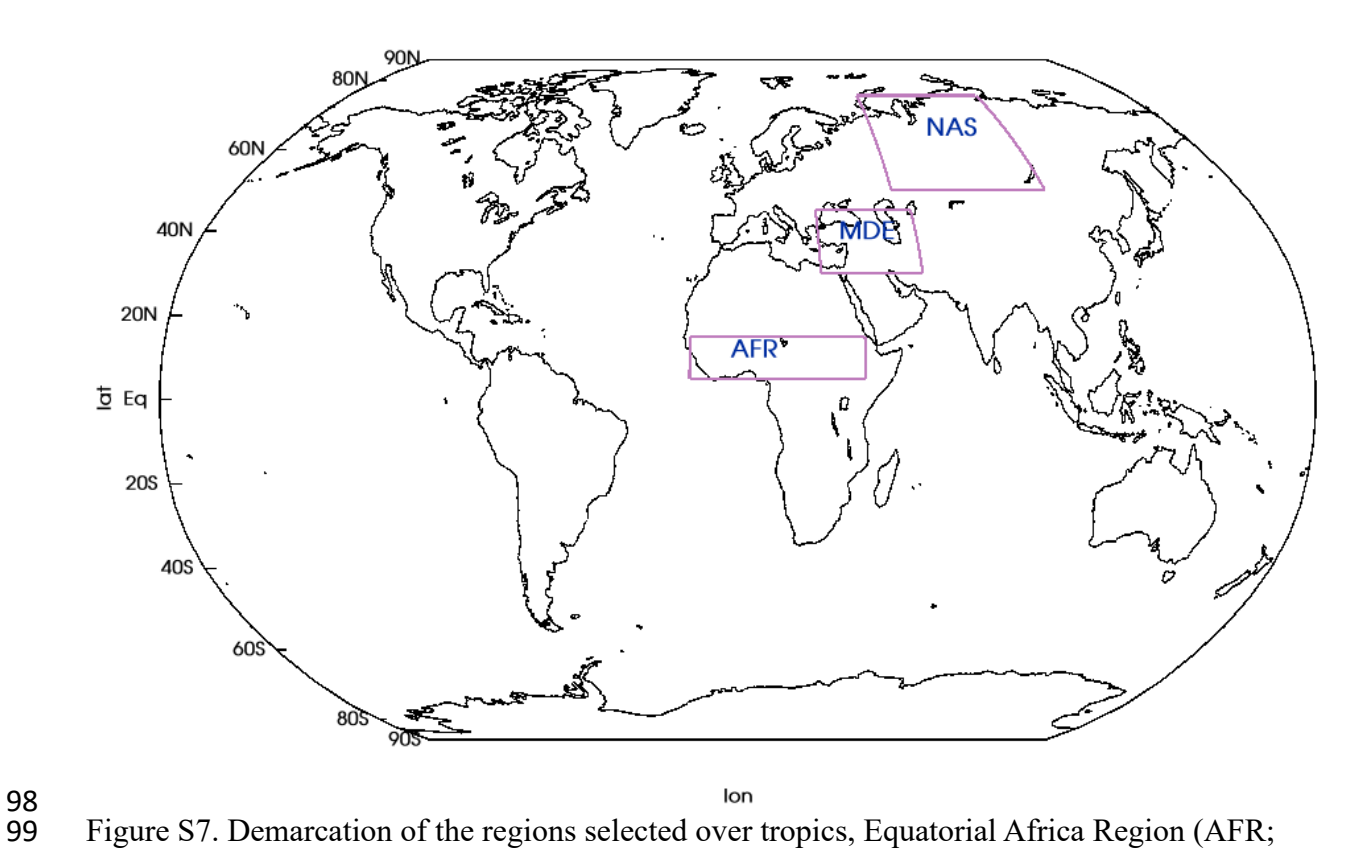


Figure S7. Demarcation of the regions selected over tropics, Equatorial Africa Region (AFR; Lat: $5^{\circ}N - 15^{\circ}N$, Lon: $15^{\circ}W - 40^{\circ}E$), mid-latitude, Middle East Region (MDE; Lat: $30^{\circ}N - 45^{\circ}N$, Lon: $27^{\circ}E - 60^{\circ}E$), and in the high latitudes, Northern Asia Region (NAS; Lat: $50^{\circ}N - 75^{\circ}N$, Lon: $55^{\circ}W - 110^{\circ}E$).

Total Irrigation Change (mm/d)

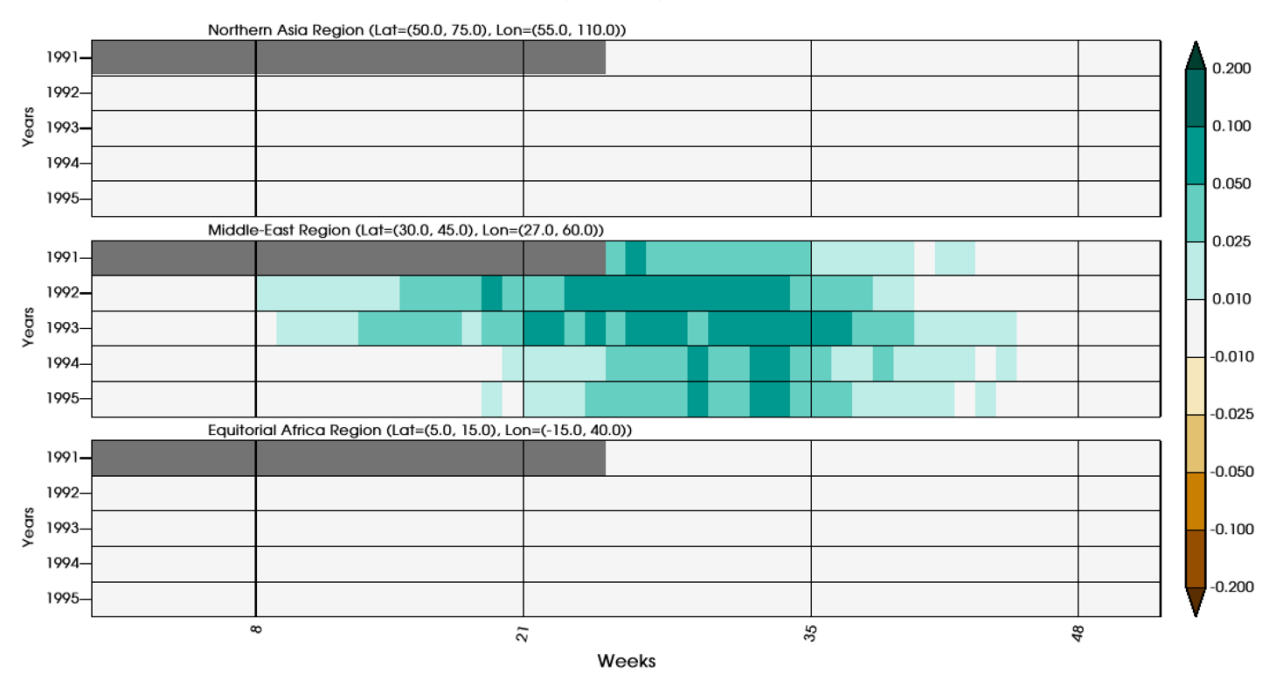


Figure S8. regionally averaged irrigation implemented in GISS modelE2.1 for the years 1991 1995.

126 S6. Vegetation distribution and GPP response

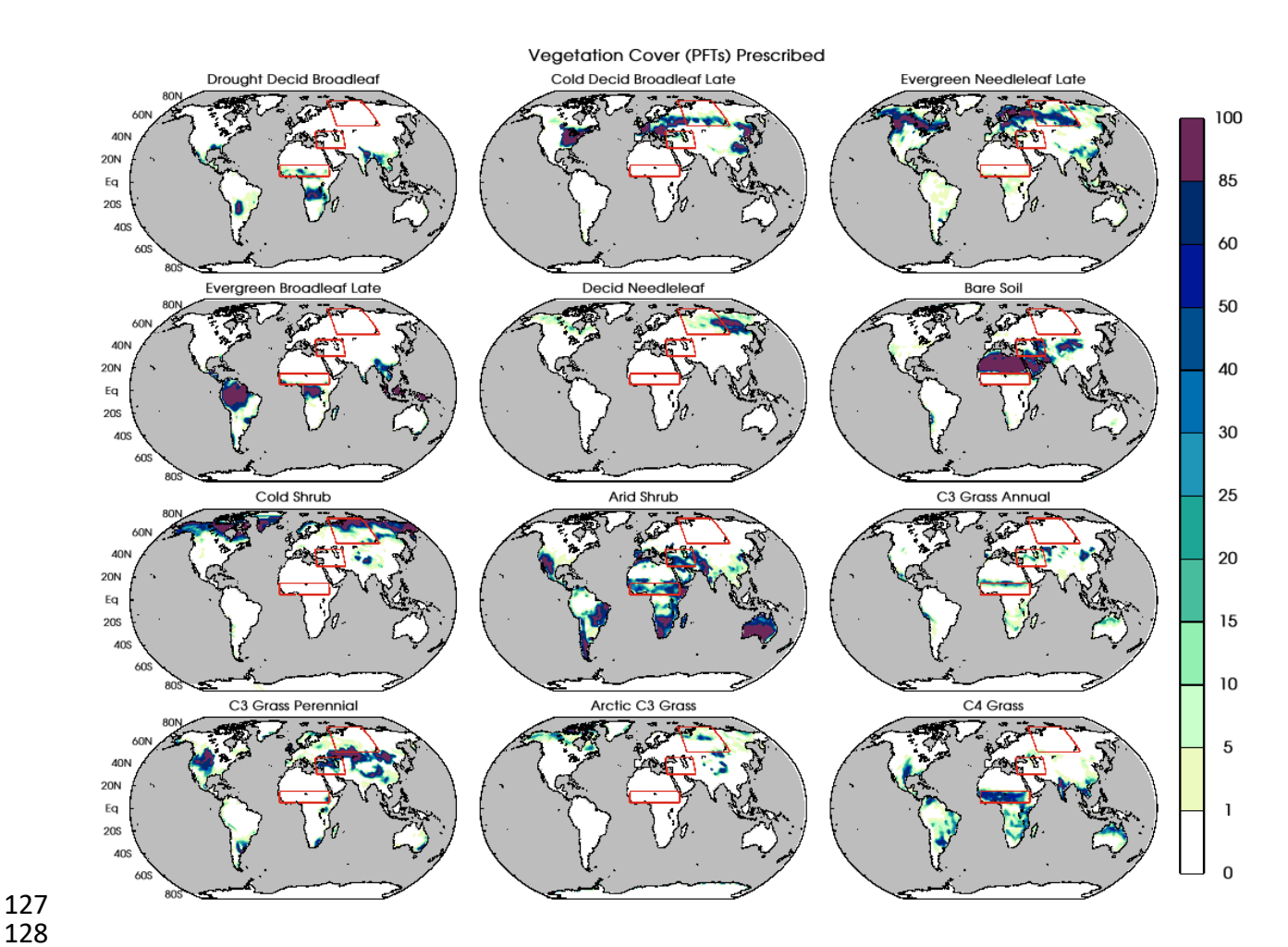


Figure S9. Percentage of grid cells for various vegetation plant functional type (PFTs) prescribed to ModelE. Red colored boxes are the various regions selected for the weekly scale analysis of drought metrices.

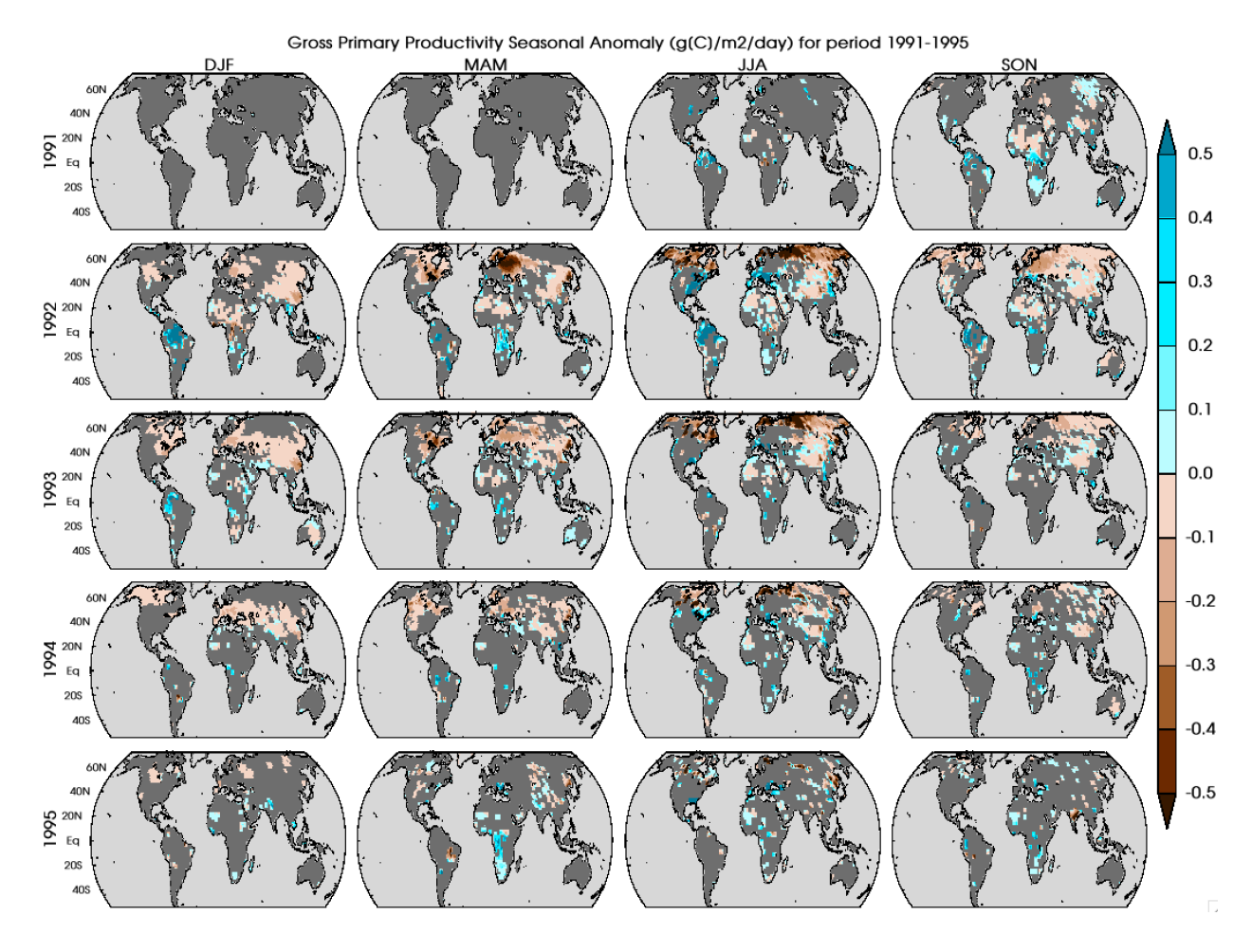


Figure S10. Seasonal Gross Primary Productivity (GPP) $(g(C)/m^2/day)$ from the year 1991 to 1995 with respect to the reference period of 1950-2014. A grey color is painted over the grid cells where the GPP anomalies are not statistically significant in comparison to the No Pinatubo (NP) ensemble. The colored areas show anomalies of PCH with respect to the climatology from 1950-2014

158 Reference:

- Bauer, S. E., Wright, D. L., Koch, D., Lewis, E. R., McGraw, R., Chang, L.-S., Schwartz, S. E.,
- and Ruedy, R.: MATRIX (Multiconfiguration Aerosol TRacker of mIXing state): an aerosol
- microphysical module for global atmospheric models, Atmospheric Chemistry and Physics, 8,
- 163 6003–6035, https://doi.org/10.5194/acp-8-6003-2008, 2008.
- Bauman, J. J., Russell, P. B., Geller, M. A., and Hamill, P.: A stratospheric aerosol climatology
- from SAGE II and CLAES measurements: 2. Results and comparisons, 1984–1999, Journal of
- Geophysical Research: Atmospheres, 108, https://doi.org/10.1029/2002JD002993, 2003.
- Bekki, S.: Oxidation of volcanic SO2: A sink for stratospheric OH and H2O, Geophysical
- Research Letters, 22, 913–916, https://doi.org/10.1029/95GL00534, 1995.
- Bingen, C., Fussen, D., and Vanhellemont, F.: A global climatology of stratospheric aerosol size
- distribution parameters derived from SAGE II data over the period 1984–2000: 1. Methodology
- and climatological observations, Journal of Geophysical Research: Atmospheres, 109,
- https://doi.org/10.1029/2003JD003518, 2004.
- 173 Colose, C. M., LeGrande, A. N., and Vuille, M.: Hemispherically asymmetric volcanic forcing of
- tropical hydroclimate during the last millennium, Earth System Dynamics, 7, 681–696,
- 175 https://doi.org/10.5194/esd-7-681-2016, 2016.
- 176 Quaglia, I., Timmreck, C., Niemeier, U., Visioni, D., Pitari, G., Brodowsky, C., Brühl, C.,
- Dhomse, S. S., Franke, H., Laakso, A., Mann, G. W., Rozanov, E., and Sukhodolov, T.:
- 178 Interactive stratospheric aerosol models' response to different amounts and altitudes of SO₂
- injection during the 1991 Pinatubo eruption, Atmospheric Chemistry and Physics, 23, 921–948,
- 180 https://doi.org/10.5194/acp-23-921-2023, 2023.
- Ramaswamy, V., Schwarzkopf, M. D., Randel, W. J., Santer, B. D., Soden, B. J., and Stenchikov,
- G. L.: Anthropogenic and Natural Influences in the Evolution of Lower Stratospheric Cooling,
- 183 Science, 311, 1138–1141, https://doi.org/10.1126/science.1122587, 2006.
- Russell, P. B., Livingston, J. M., Pueschel, R. F., Bauman, J. J., Pollack, J. B., Brooks, S. L.,
- Hamill, P., Thomason, L. W., Stowe, L. L., Deshler, T., Dutton, E. G., and Bergstrom, R. W.:
- 186 Global to microscale evolution of the Pinatubo volcanic aerosol derived from diverse
- measurements and analyses, Journal of Geophysical Research: Atmospheres, 101, 18745–18763,
- 188 https://doi.org/10.1029/96JD01162, 1996.
- 189 Stenchikov, G. L., Kirchner, I., Robock, A., Graf, H.-F., Antuña, J. C., Grainger, R. G., Lambert,
- 190 A., and Thomason, L.: Radiative forcing from the 1991 Mount Pinatubo volcanic eruption,
- Journal of Geophysical Research: Atmospheres, 103, 13837–13857,
- 192 https://doi.org/10.1029/98JD00693, 1998.